

Towards a greener electrosynthesis: pairing machine learning and 3D printing for rapid optimisation of anodic trifluoromethylation

Nipun Kumar Gupta^{1,6,†}, Yilin Guo^{2,†}, Soon Yee Chang^{2,†}, Jing Lin^{3,†}, Zi Hui Jonathan Khoo^{1,6}, Riko I Made¹, Zi En Ooi¹, Carina Yi Jing Lim¹, Chow Hern Lee⁴, M. Sivapaalan⁵, Yee-Fun Lim^{1,6}, Edwin Khoo^{*,3}, Lu Wen Feng^{2,*}, Yanwei Lum^{1,*}, Albertus D. Handoko^{1,6,*}

¹Institute of Materials Research and Engineering (IMRE), Agency for Science, Technology and Research (A*STAR), 2 Fusionopolis Way, Innovis, Singapore 138634

²NUS Centre for Additive Manufacturing (AM.NUS), E3-02-07, E3, Engineering Block 2, Engineering Drive 3, Singapore 117581.

³Institute for Infocomm Research (I²R), Agency for Science, Technology and Research (A*STAR), 1 Fusionopolis Way, Connexis, Singapore 138632, Singapore

⁴School of Chemical and Biomedical Engineering, Nanyang Technological University, 50 Nanyang Avenue, Singapore 639798

⁵School of Materials Science and Engineering, Nanyang Technological University, 50 Nanyang Avenue, Singapore 639798

⁶Institute of Sustainability for Chemicals, Energy and Environment, Agency for Science, Technology and Research (A*STAR), 1 Pesek Road, Jurong Island, Singapore 627833, Singapore

*Authors to whom correspondence should be addressed: edwin_khoo@i2r.a-star.edu.sg ;

mpelwf@nus.edu.sg ; lum_yanwei@imre.a-star.edu.sg ; Handoko_Albertus@isce2.a-star.edu.sg

†These authors contributed equally.

Keywords: 3D printing, Bayesian Optimisation, Machine Learning, Kinetic Modelling, Anodic Trifluoromethylation, Electro-organic synthesis

S1: Flow electrofluorination setup and automation

A schematic of the flow reaction setup is shown in **Figure S1A**. The flow reaction setup consists of various components that work in tandem. The prepared reagent is stored in the reagent bottles and is degassed under Ar gas to remove the dioxygen. Pump 1 draws the reactants from the reagent bottle into the Waters degasser, where any traces of air are expelled from the reactant mixture. Pump 1 then pushes the reactant mixture into the flow cell, where the actual reaction occurs. The outflow from the flow cell is collected with a Foxy fraction collector. An Ivium XRi potentiostat controls the cell reaction. Pump 2 controls the water flow from the recirculating water cooler to maintain the cell temperature. The setup is automated: Pumps 1 and 2, fraction collector and the water temperature of the recirculating water cooler are controlled with a LabView interface.

The precise control of the working electrode's potential can be achieved using a three-electrode configuration; however, the presence of a reference electrode complicates the reactor design. Thus, we used a two-electrode design, and all investigations herein are conducted. To prevent the leeching of metal ions from a metallic, the direction of the current flow needs to be controlled, and so the input herein is current controlled rather than voltage controlled.

A schematic of the flow cell is shown in **Figure S1B**. The rigid PEEK flow cell casing encloses the flow paths, gaskets, and electrodes within it. A graphite plate is used as the anode, and various 3D-printed patterned stainless-steel (SS) plates are used as the cathodes in this study. All the cell components were manually assembled and securely held in the PEEK casing with nuts and bolts. The reactant enters the cell from the anode side and exits from the cathode side. A recirculating water cooler controlled the cell temperature, the water loop was isolated from the reactant pathway in the cell with a flow path, and a Ti plate was put behind the graphite anode to ensure a uniform temperature was maintained across the anode.

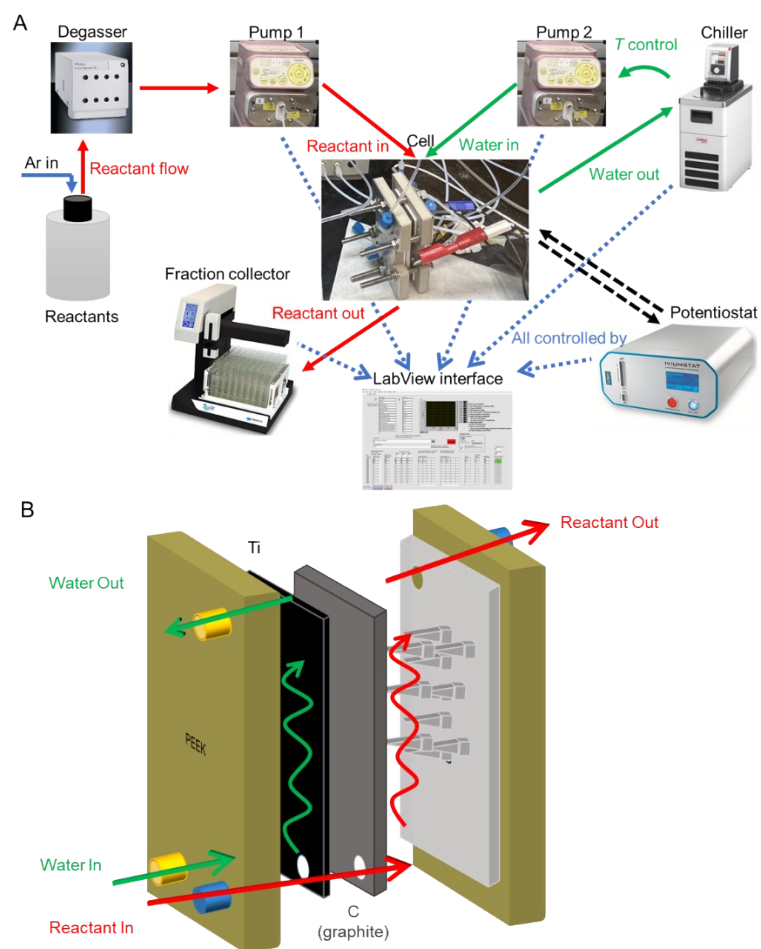


Figure S1: (A) A schematic representation of the flow reaction setup. All the components of the setup are labelled. Briefly, the reactant mixture is pumped from the reagent bottle to the degasser and then through the pump into the flow cell, where the actual reaction occurs, and the fraction collector collects the outflow. A chiller maintains the cell temperature, and a separate pump controls the inflow and outflow of the water. A potentiostat is used to apply the electrical current/ voltage necessary to drive the reaction. The pump flow rate(s), fraction collector's fraction volume and number, input current and voltage, and the water temperature in the chiller are controlled with a LabView interface. (B) A schematic representation of the flow cell. The cell consists of a PEEK casing to support the C (graphite) anode and the 3D-printed SS cathodes. A Ti plate is added behind the graphite plate for mechanical support and to ensure that the entire anode maintains a uniform temperature. The water and the reactants are not allowed to come into contact in the cell, and the flow path (not shown here) is used to direct the flow of the reactants and water inside the cell.

S2: Fourier Transformed AC Voltammetry and fittings

Fitting of numerical simulation of the fourth harmonics IFT FTAC of caffeine, NaSO_2CF_3 and reagent mixtures are shown in **Figure S2**. The fitted parameters are shown in **Table S1-S3**.

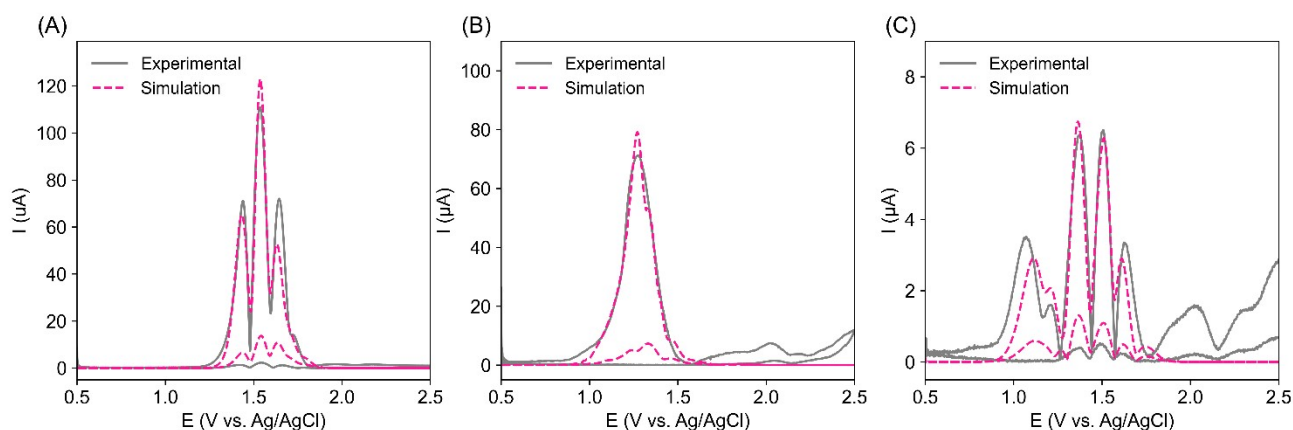


Figure S2: Numerical fittings of fourth harmonics IFT FTAC (broken pink line) overlaid on experimental data of (A) caffeine, (B) NaSO_2CF_3 , and (C) caffeine + NaSO_2CF_3 . All reagents are dissolved in acetonitrile with TBAP as a supporting electrolyte.

Table S1: FTAC parameter fitting for TBAP + Caffeine.

Reaction	E^0 V	λ eV	k_s cm/s	k_{eq}	k_f	D cm ² /s	C_{init}/C_{anal} mol/L
$\text{Ox} + 2e \rightleftharpoons \text{Red}$	1.301	100.000	5.75×10^{-8}				
$\text{Ox}_2 + 2e = \text{Ox}$	1.627	50.000	4.52×10^{-3}				
$\text{Ox}_2 \rightarrow \text{P}$					14.31		
Ox						8.34×10^{-7}	0
Ox ₂						NA	0
P						NA	0
Red						2.96×10^{-10}	0.050

Table S2: FTAC parameter fitting for TBAP + NaSO_2CF_3 .

Reaction	E^0 V	λ eV	k_s cm/s	k_{eq}	k_f	D cm ² /s	C_{init}/C_{anal} mol/L
$\text{Ox} + e \rightleftharpoons \text{Red}$	1.259	0.365	9.87				
$\text{Ox}_2 + 2e \rightleftharpoons \text{Ox}$	1.532	16.384	3.11×10^8				
$\text{Ox}_2 \rightarrow \text{P}$					$5.34 \times 10^{+11}$		
$\text{Red}_2 = \text{Red}$				0.037	$1.36 \times 10^{+14}$		
Ox						2.78×10^1	0
Ox ₂						1.69×10^{-5}	0
P						NA	0
Red						2.47×10^1	0.050

Red2	6.38×10^{-3}	0.010
------	-----------------------	-------

Table S3: FTAC parameter fitting for TBAP + Caffeine + NaSO₂CF₃.

Reaction	E ⁰ V	λ eV	k _s cm/s	k _{eq}	k _f	D cm ² /s	C _{init} /C _{anal} mol/L
Ox + e <= Red	1.662	0.654	9.83×10^{-5}				
Ox2 + 2e <= Ox	1.200	0.356	1.30×10^{-5}				
Ox3 + e = Red2	1.212	0.195	3.69×10^{-5}				
Ox4 + e = Ox3	1.204	0.027	4.00×10^{-5}				
Ox2 --> P					3.13		
Ox4-->P2					4.30×10^6		
Ox						1.81×10^{-6}	0
Ox2						4.00×10^{-5}	0
P						NA	0
Red						3.17×10^{-11}	0.005
Ox3						5.86×10^{-10}	0

S3: NMR quantitation:

A JEOL JNM ECA500 system was used in this study to record the NMR spectra. The NMR quantitation of the product mixture was done with an internal standard (IS)¹. The ¹H (or ¹⁹F) NMR peak intensity of a specie is directly co-related to its concentration and is inversely correlated to the number of ¹Hs (or ¹⁹Fs) responsible for the said peak. So, we can co-relate the intensity of the analyte (I_A), the number of protons responsible for the analyte peak (N_A) with the concentration ($[analyte]$) with the IS's peak intensity (I_{IS}), the number of protons for the IS peak (N_{IS}) with the concentration of the IS ($[IS]$) with this relationship:

$$[analyte] = \frac{[IS] \times I_A \times N_{IS}}{N_A \times I_{IS}}$$

We characterised the reaction mixture with NMR to identify the concentration of the product and unreacted reactant species. For this, we collected 5 fractions of the identical volume of the outflow from the cell to ensure that the collected final volume for all the reactions would be comparable, irrespective of the flow rate. We measured the NMR of the 5th fraction for all the reactions.

We tested the stability of the reactants in extreme pH by recording the NMR spectra of the reactants in pH 0.5 and 15.5, as presented in Fig. S2. The caffeine concentration was set at 50 mM, and the sodium trifluoromethanesulphinate (NaSO_2CF_3) concentration was set at 100 mM to mimic the actual reaction conditions. The solutions were prepared in 100 mM tetrabutylammonium perchlorate ($\text{N}(\text{C}_2\text{H}_9)_4\text{ClO}_4$, TBAP) in a 10:1 acetonitrile: water solvent system. The caffeine and NaSO_2CF_3 concentration were quantified with dimethyl sulphoxide (DMSO) and 4,4'-difluorobenzophenone (DFB) as internal standards.

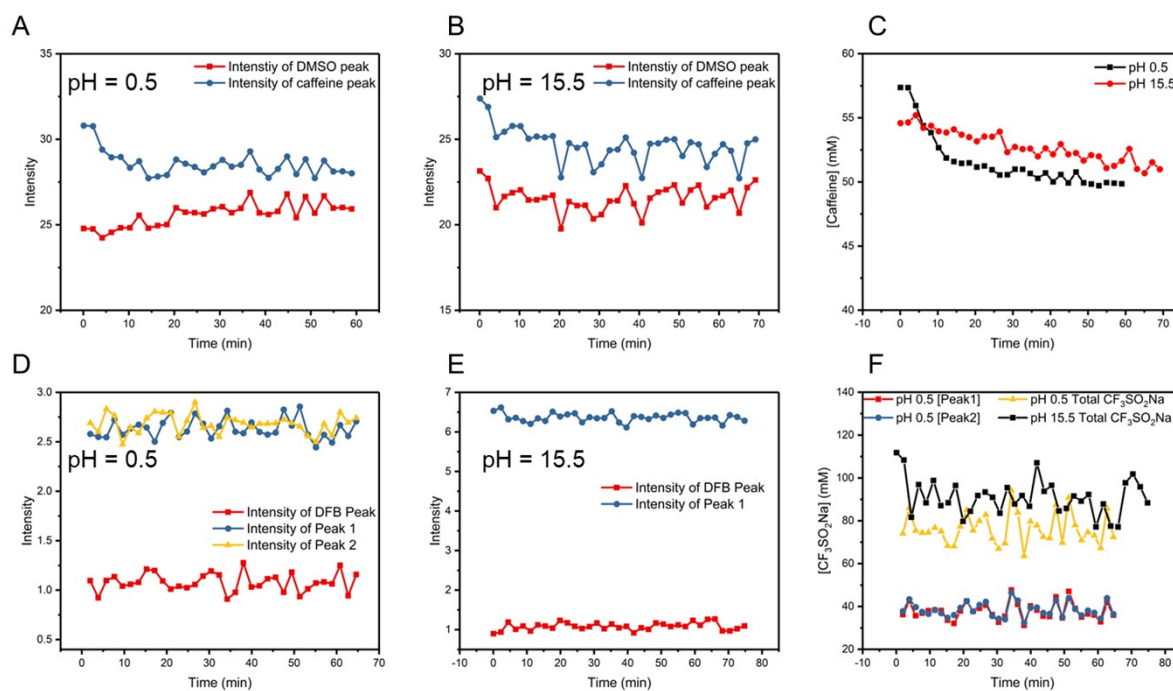


Figure S3: Peak intensity as a function of time (in min) for caffeine species in (A) acidic pH and (B) basic pH obtained from ^1H NMR, and the peak intensity for SO_2CF_3^- species in (C) acidic and (E) basic pH as a function of time obtained from ^{19}F NMR. The intensity is used to obtain the concentration profile of the (C) caffeine and (F) NaSO_2CF_3 at acidic and basic pH.

S4: Electrode choice, Preliminary study, and Characterisation of the side-products

The X-ray diffraction was measured using Bruker D8 Discover goniometer equipped with a capillary focused $I\mu\text{S } 2.0 \text{ Cu K}\alpha$ X-ray source (50 kV, 1000 μA). The incoming beam is focused to 1 mm radius using a pinhole collimator. Vantec 500 with Xe micro gap 2D detector positioned at 420 mm radius was used as an X-ray detector.

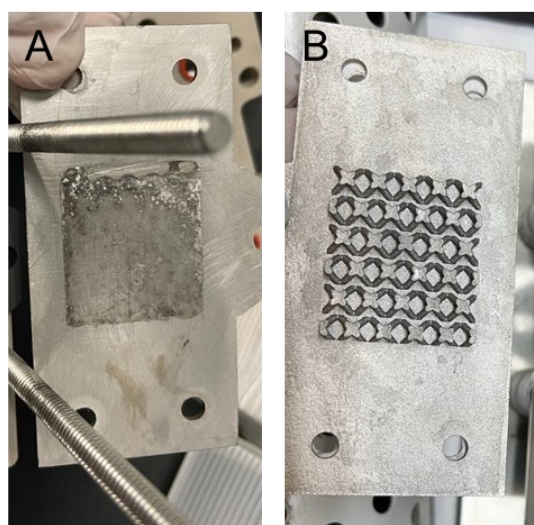


Figure S4: Pictures of the (A) flat SS and (B) 3D-printed BCC-6mm SS cathodes after a trifluoromethylation reaction under identical flow experimental conditions. Flat SS electrode shows much more significant fouling and deposit.

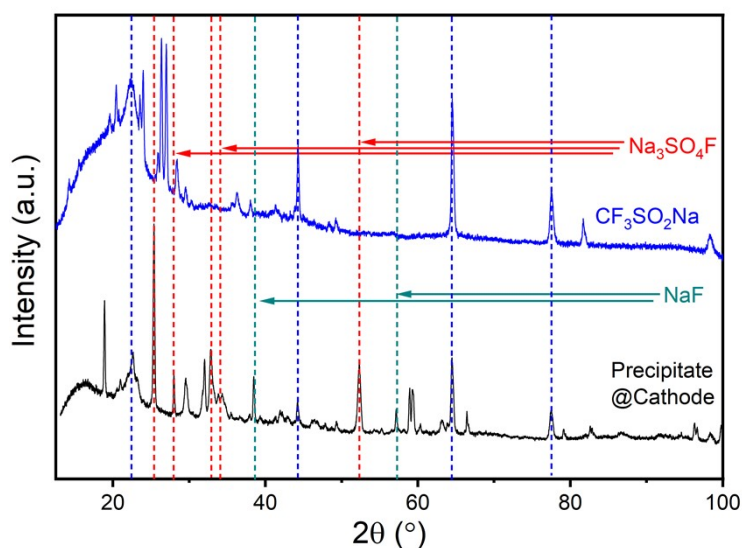


Figure S5: Powder XRD of the precipitate formed at the flat SS cathode surface.

Experiments to confirm the gas phase side products from the trifluoromethylation reaction:

The gaseous phase products were characterised by an Agilent 5975 GCMS system. We used a divided cell setup to identify the gaseous side-products of the reaction. We used a Celgard® membrane to isolate the anode and the cathode compartments and used a Flat SS plate as the cathode. To collect the gas, the setup described in the main text was slightly modified to capture the gas. We conducted the reaction with a slow flow rate of 0.25 mL min^{-1} , a steady 60 mA input current and $T = 65 \text{ }^\circ\text{C}$ to maximise the amount of the gas produced in the reaction. A 50 mL glass bottle was capped with HPLC GL 45 delivery cap (with $3 \times \frac{1}{4}$ -28 UNF inlet) was rinsed with dinitrogen to expel the air. One inlet of the cap was blocked, the second was connected to the cell outflow tube to collect the product mixture, and the third one was connected to a 50 mL gas-tight syringe. The reaction was run continuously for an hour to produce enough gaseous side products so they could be detected by a GC-MS detector.

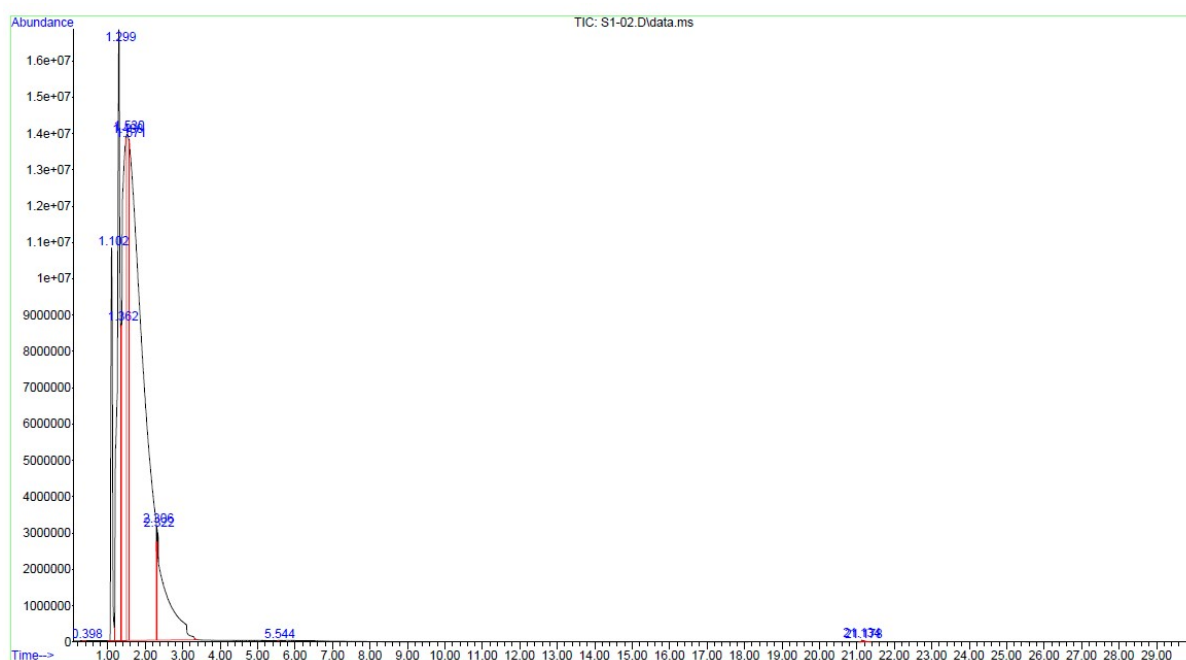


Figure S6: The gas chromatograph for the gaseous side-products collected from the anode compartment.

The gas chromatograph is presented for the gaseous side products is presented in Fig. S6. We see a steady evolution of peaks from the start (0 min) to 5 min; another peak is identified at 21 min. The MS for the gas chromatograph is presented next. Briefly, we detect acetonitrile (molecular weight:

41 g mol⁻¹), fluoroform (molecular weight: 69 g), hexafluoroethane (molecular weight: 138 g) and carbon dioxide (molecular weight: 44 g) between 0 and 5 min, and unreacted caffeine (molecular weight: 194 g) is detected at 21 min.

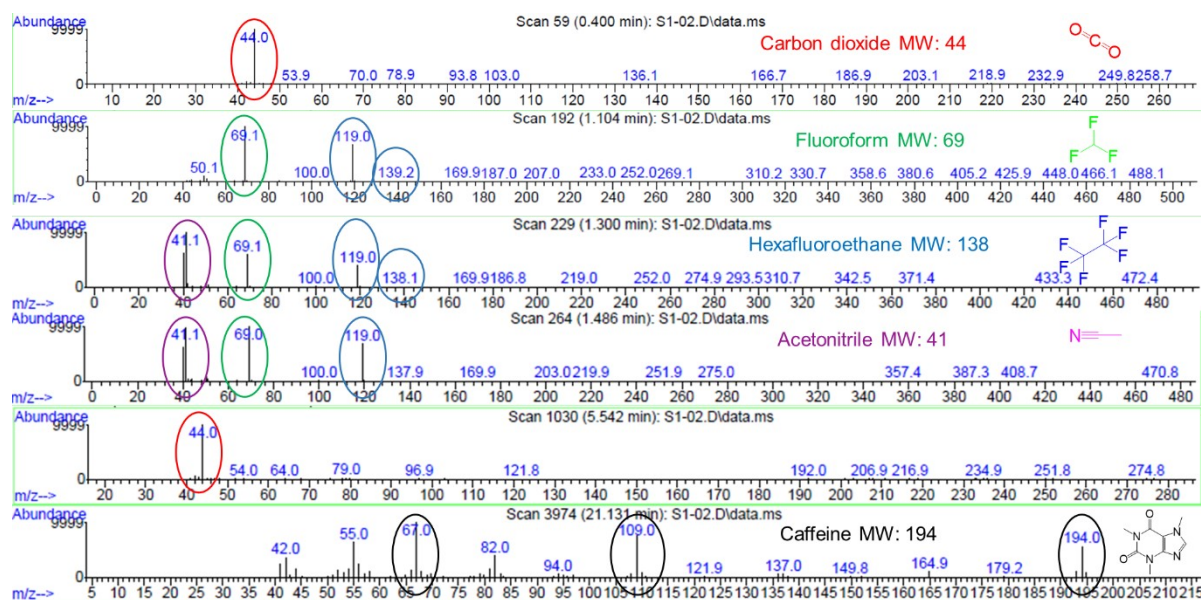


Figure S7: Mass spectra of multiple peaks of interest observed in Figure S6. The corresponding retention time is written on the top of each panels: Scan 59 (possible CO₂ fragment) = 0.400 min; Scan 192 (fluoroform) = 1.104 min; Scan 229 (hexafluoroethane) = 1.300 min; Scan 264 (acetonitrile) = 1.486 min; Scan 1030 (possible CO₂ fragment) = 5.542 min; Scan 3974 (Caffeine) = 21.131 min.

S5: CFD modelling

Design and geometry parameters of planar electrode and BCC electrode are described in **Table S4**. CFD simulation conducted on BCC-6mm and the planar electrode at 0.25 ml min^{-1} flow rate indicated that both designs have a uniform distribution of velocity (**Table S5-1**). However, it is observed that the BCC-6mm electrode increases the maximum velocity magnitude fluid flow to around $6 \times 10^{-4} \text{ m s}^{-1}$, almost double that in the planar electrode (**Table S5-2**). The higher velocity is known to improve the solid deposition situation in the electrochemical reactor. Compared to other

In addition to velocity distribution, the simulation of the residence time distribution (RTD) curve, which describes the tracer distribution at the outlet in a certain period can be assessed using this formula:

$$E(t) = C(t) / \left(\int_0^{\infty} C(t) dt \right)$$

To compare the different electrodes with different residence times, the dimensionless RTD can be calculated by $E(\theta)$, where θ is the dimensionless residence time t/t_{mean} . As shown in **Figure S8**, the simulated RTD curve as a function of the dimensionless residence time of the BCC-6mm electrode is compared with the planar electrode. It can be observed that all the RTD curves are asymmetric. At both inlet flow rates of 0.25 ml/min and 1.5 ml/min , the maximum $E(\theta)$ has been reached before the dimensionless residence time $\theta = 1$, indicating some fraction of the fluid reaches the exit zone more quickly. However, at a low inlet flow rate (0.25 ml min^{-1}), BCC 6mm exhibit a more symmetric RTD curve than the planar electrode, indicating a slightly more uniform flow.

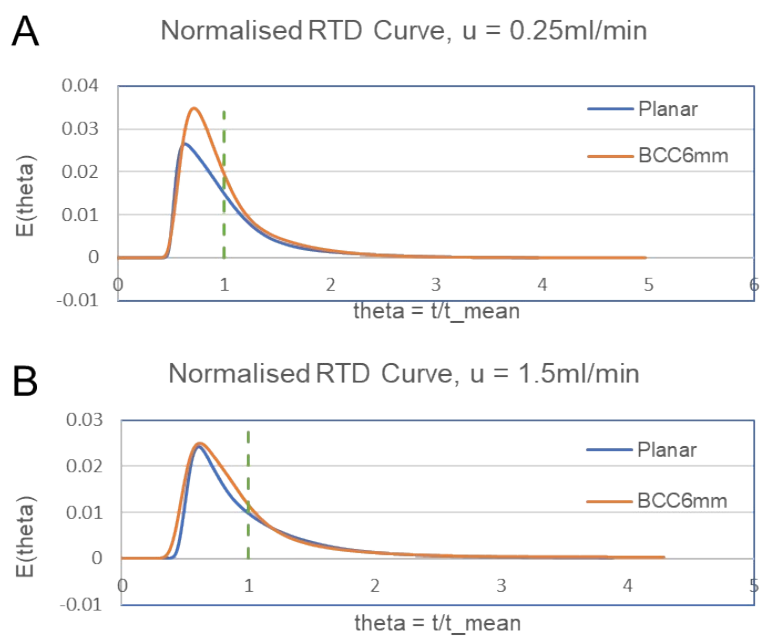


Figure S8: The figure compares simulated RTD curves of the planar electrode and BCC 6mm electrode at an inlet flow rate of 0.25 ml min^{-1} and 1.5 ml min^{-1} .

Table S4: Design and geometry parameters of planar electrode and BCC electrode.

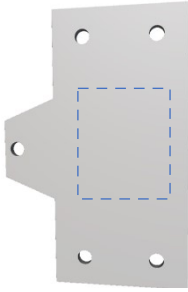

	(a) Planar electrode	(b) BCC (6mm unit cell) electrode
Schematic		
Unit cell size (mm)	NA	6
Strut diameter (mm)	NA	1.5
Porosity ^a	100%	75%
Surface area (mm ²)	1050	3395

Table S5: Velocity distribution and velocity profile in the channel width of parallel plate reactor from CFD simulation.

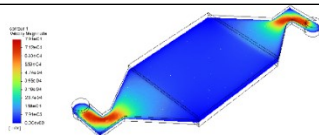
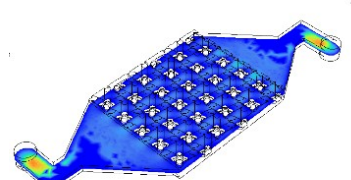
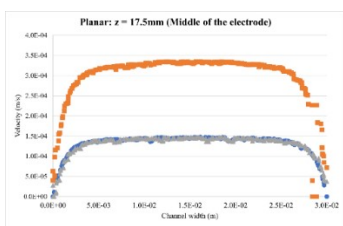
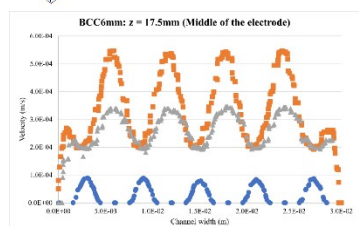
	Planar electrode	BCC (6mm unit cell) electrode
Velocity distribution at 0.25 ml min ⁻¹ flow rate		
Velocity profile at the height of (o) 0.5mm, (□) 2mm, (Δ) 3.5mm in y-coordinates.		
Mean particle residence time (stdev) in s	278 (875)	322 (613)

Table S6: Summary electrode design alternative surface area and particle residence times

Design (inlet flow rate = 1.5ml/min)	Surface Area [mm ²]	Particle residence time [s]	
		Mean	St Dev
Planar Plate Electrode	1050	278	875
BCC 6mm staggered	3198	322	613
BCC 6mm removed 1 st row	2859	280	525
BCC 6mm removed 3 rd and 4 th row	2525	298	668
BCC 6mm rotate 1 st row	3031	276	569

Table S7: Summary of the experiments with electrode configuration

No	Cathode	Flow rate	ON Current	OFF Current	Duty cycle	<i>T</i>	<i>F</i>	¹ H NMR unreacted Caffeine ^a	¹ H NMR CF ₃ product ^a	¹⁹ F NMR unreacted CF ₃ SO ₂ Na ^b	¹⁹ F NMR product ^b	Yield	Production rate
		mL min ⁻¹	mA	mA		°C	Hz	mM	mM	mM	mM	%	μmol min ⁻¹
1	Flat SS	0.50	60	-60	0.90	30	4.55	38.32	7.15	49.79	7.63	14.78	3.82
2	Flat SS	0.50	60	20	0.50	30	100.00	42.90	7.15	59.90	7.34	14.49	3.67
3	BCC-6mm SS	0.50	60	-60	0.90	30	4.55	38.04	10.01	42.64	9.16	19.17	4.58
4	BCC-6mm SS	0.50	60	20	0.50	30	100.00	40.04	8.58	57.04	8.39	16.97	4.20
5 ^c	BCC-6mm SS	0.25	60	-	-	65	-	31.46	12.01	15.93	11.54	26.40	2.89

- All reactions were done with 100 mM TBAP in 10:1 acetonitrile: H₂O as electrolyte with Graphite as the working electrode in chronoamperometry mode. The nominal concentrations of the CF₃SO₂Na and caffeine were set to 100 mM and 50 mM
- ^aThe estimation was done with 14.3 mM DMSO in deuterated acetonitrile as the internal standard with the 3.9 ppm peak of caffeine and 4.1 ppm peak of 1,3,7-Trimethyl-8-(trifluoromethyl)-3,7-dihydro-1H-purine-2,6-dione product (**I**)
- ^bThe estimation was done with 14.3 mM DFB in deuterated acetonitrile as the internal standard with ~63 ppm peak of **I** and ~79 ppm and ~88 ppm for the CF₃SO₂Na
- ^cThe experiment was conducted under constant current chronoamperometry (DC chronoamperometry)

S6: Reaction Optimisation

ML Optimisation

We leverage our ML framework for optimising the six input parameters with constraints. (**Figure S9**). To start off, prior sampling was done with the experimental parameters generated via the Latin Hypercube algorithm (LHS)² as implemented in scikit-optimize³. We chose LHS mainly to maximise the range of exploration with the minimum number of samples, where we also tried to minimise the overlap between the experimental conditions.

Constructing Surrogate Model

Given the input parameters, we then construct a surrogate ANN – as implemented in Keras/Tensor Flow framework as an estimator for the target output. ANN was chosen primarily due to their better handling of multiple input parameters. Further, prior experimental results on similar reaction and reactor system demonstrated better stability and have a higher chance for prediction/extrapolation (Figure S9).

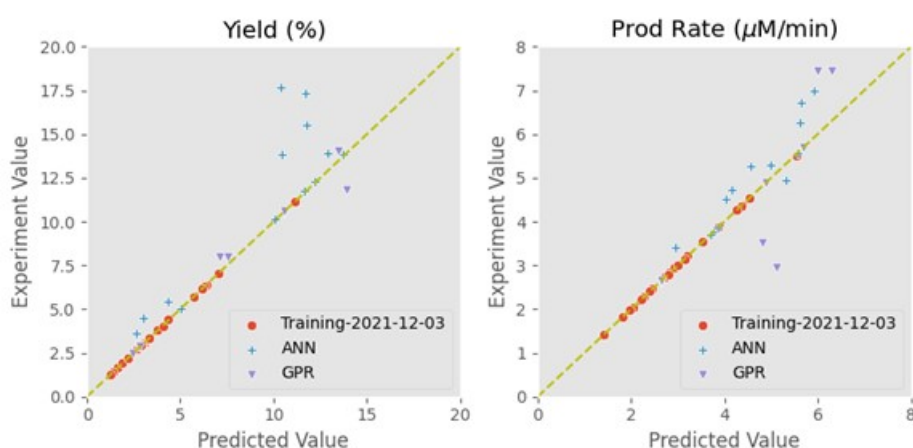


Figure S9: Prior experimental optimisation with similar reaction and system, comparing GPR (purple down triangle sign) and ANN (blue plus sign).

However, determining the structure of the neural networks requires hyperparameter (HP) tuning that is non-trivial with non-unique solutions. Here, we implement Bayesian Optimisation for selecting the hyperparameters as implemented in scikit-optimize.

We generate two models to predict yield, and production rate, respectively. Considering the small number of data points present in the training dataset, we adopt the "leave one out" strategy for cross-validation of the model training and evaluations. We save the models in pickled form – hdf5 format – to be reused and re-trained as new priors are generated.

Optimisation

We generate three types of suggestions for the subsequent experiments, and they are: search for a better yield, a better production rate, and both. The first two objectives were encapsulated as objective functions that are to be minimised as input in Bayesian Optimisation (BO) as implemented as `gp_minimize` in scikit-optimize. The third is a multi-objective problem that we scalarised to a single objective. The suggested experimental parameters from optimisation algorithms are then tested with the actual experiments. The prior is updated with the results of the new experiments, and the three models are re-trained for the next iteration.

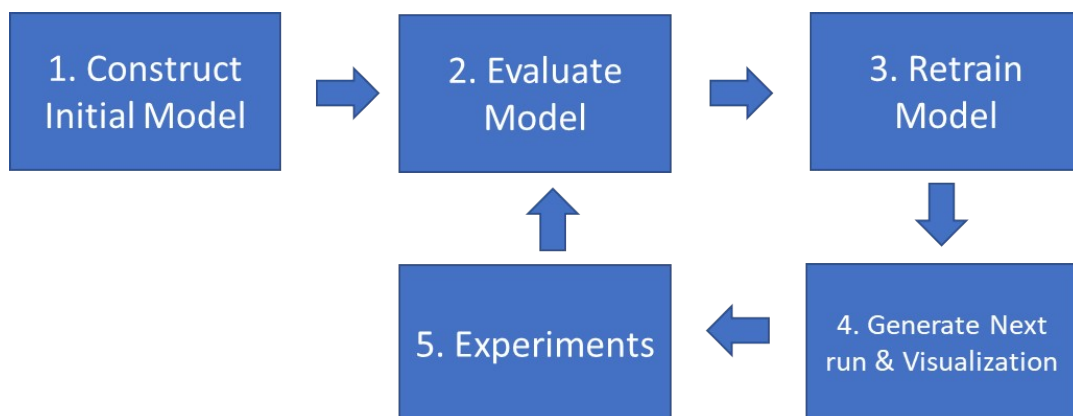


Figure S10: The framework for the ML-assisted optimisation

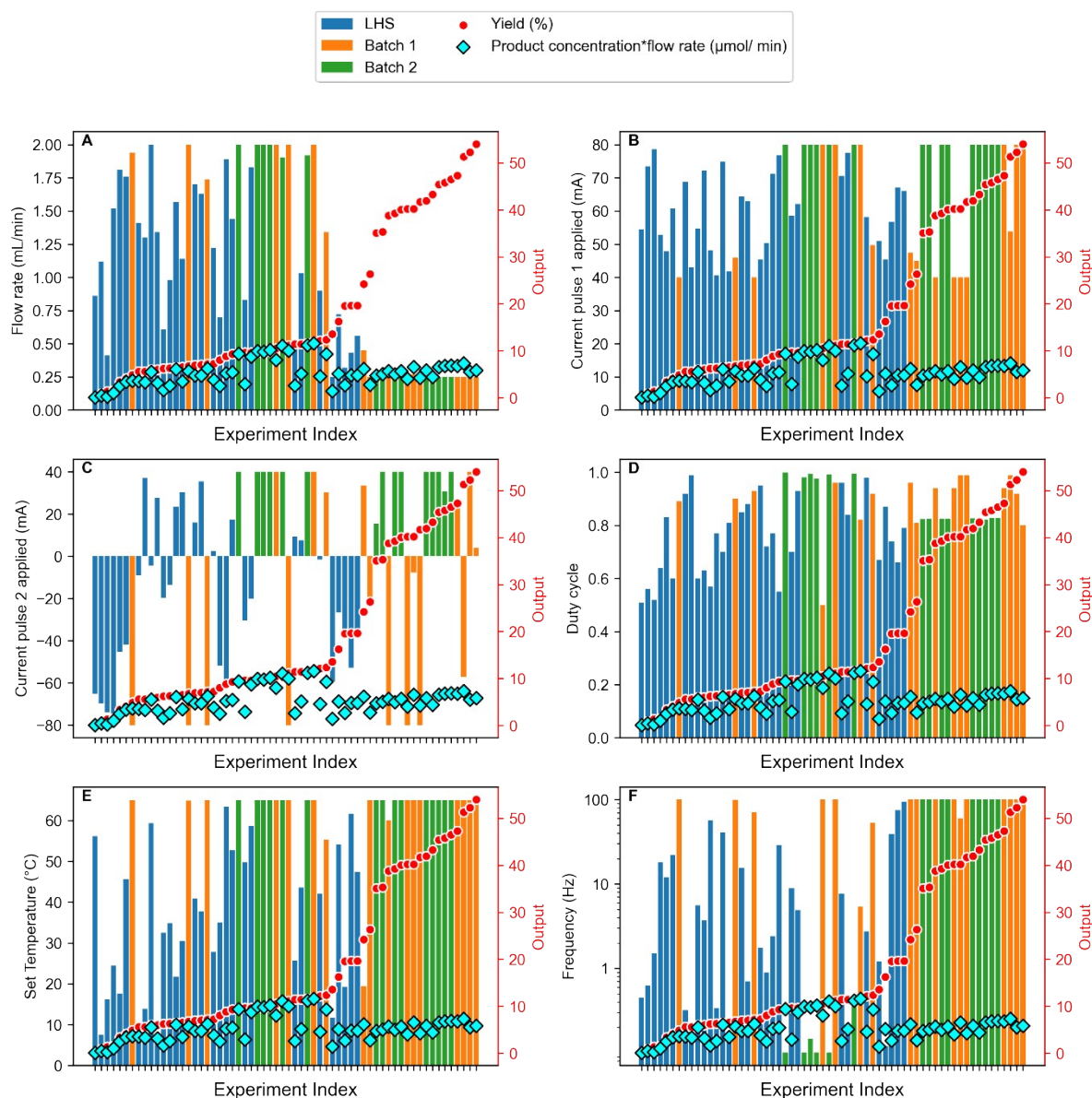


Figure S11: Optimisation evolution for both yield (red circles, right axis) and production rate (cyan diamonds, right axis) objectives with respect to (A) flow rate, (B) current pulse 1, (C) current pulse 2, (D) duty cycle, (E) set temperature, and (F) frequency. The objective values are plotted as the secondary axis for each input parameter. The colour code represents the optimisation batch, with blue representing the initial sampling, orange for Batch 1 and green for Batch 2.

S7: Reaction Data

Table S7: Summary of the initial sampling parameters generated with the Latin Hypercube (LHS)

Serial Number	Flow rate	ON Current	OFF Current	Duty cycle	<i>T</i>	<i>F</i>	¹ H NMR unreacted Caffeine ^a	¹ H NMR CF ₃ product ^a	¹⁹ F NMR unreacted CF ₃ SO ₂ Na ^b	¹⁹ F NMR product ^b	Yield	Production rate	pH
	mL min ⁻¹	mA	mA		°C	Hz	mM	mM	mM	mM	%	μmol min ⁻¹	
1	1.34	72.19	27.82	0.63	6.27	3.71	40.61	3.15	67.43	2.86	6.01	3.83	2.00
2	1.12	73.49	-69.55	0.56	7.54	0.63	43.47	0.57	78.21	0.29	0.86	0.32	3.40
3	1.41	68.87	-9.13	0.92	10.74	0.32	41.47	2.86	64.00	2.77	5.63	3.90	2.30
4	0.25	50.95	-59.39	0.67	11.76	1.20	35.75	6.86	62.57	6.68	13.54	1.67	2.50
5	1.30	42.98	37	0.99	13.88	0.18	38.61	2.86	67.24	2.77	5.63	3.60	3.00
6	0.41	78.69	-73.94	0.52	16.14	1.50	44.04	0.57	78.88	0.76	1.34	0.31	4.50
7	1.81	47.77	-45.29	0.83	17.61	12.01	39.47	1.72	72.30	1.72	3.43	3.11	3.80
8	0.32	56.77	-39.1	0.74	19.24	39.11	30.89	10.01	37.39	9.54	19.55	3.05	4.10
9	1.57	74.92	23.44	0.7	21.71	40.97	39.18	3.15	64.86	3.34	6.48	5.24	2.20
10	1.52	52.8	-78.63	0.64	24.39	18.07	40.61	0.57	78.40	0.95	1.53	1.45	3.20
11	0.53	70.55	9.27	0.96	25.7	7.69	34.32	5.72	37.77	5.72	11.44	3.03	1.40
12	1.22	45.38	2.44	0.95	27.78	1.75	40.04	3.72	63.52	3.53	7.06	4.31	2.30
13	1.14	41.78	30.43	0.81	30.54	0.14	37.47	3.15	64.38	3.43	6.58	3.91	2.60
14	0.61	48.13	-19.88	0.57	32.48	56.15	38.90	3.15	70.77	3.05	6.20	1.86	2.80
15	0.98	40.59	-13.41	0.77	34.84	0.34	38.90	3.15	65.81	3.15	6.29	3.08	2.90
16	0.70	50.3	-51.98	0.72	35.03	0.90	38.04	4.00	66.19	4.01	8.01	2.80	3.20
17	1.63	63	35.48	0.88	37.79	0.70	37.47	3.43	65.05	3.62	7.06	5.91	3.10
18	1.70	64.31	15.98	0.85	40.88	15.51	39.75	3.43	67.53	3.53	6.96	6.00	3.80
19	0.90	58.2	-1.57	0.98	42.07	2.74	34.32	6.01	53.60	6.10	12.11	5.49	3.70
20	1.03	77.5	7.56	0.84	43.57	0.22	31.46	5.72	48.26	5.72	11.44	5.89	3.50
21	1.76	60.77	-41.87	0.6	45.68	21.93	41.76	2.00	71.34	2.10	4.10	3.69	3.80
22	0.56	66.07	-34.72	0.79	47.4	94.42	32.89	10.01	48.26	9.63	19.64	5.39	3.90
23	0.83	58.7	-30.53	0.7	49.76	8.89	37.18	4.86	70.20	4.77	9.54	3.96	3.80
24	1.44	76.9	17.34	0.55	52.75	28.98	41.76	4.58	86.70	4.77	9.35	6.87	2.30
25	0.72	45.32	-26.57	0.87	54.21	0.12	37.47	8.29	76.02	7.92	16.21	5.70	2.50
26	0.86	54.46	-65.3	0.51	56.17	0.45	46.05	0.00	83.84	0.10	0.10	0.08	4.80
27	1.83	62.16	-20.11	0.93	58.72	4.88	42.61	4.86	72.58	4.77	9.63	8.73	2.20
28	2.00	54.72	-4.51	0.6	59.32	5.56	42.04	3.15	75.16	2.86	6.01	5.72	2.60
29	0.43	67.06	-52.81	0.66	61.64	74.46	36.89	10.01	67.63	9.63	19.27	4.14	2.70
30	1.89	71.2	-61.89	0.77	63.37	2.40	40.04	4.29	76.59	4.58	9.16	8.65	2.30

- All reactions were done with 100 mM TBAP in 10:1 acetonitrile: H₂O as electrolyte with Graphite as the working electrode and BCC-6mm SS as the counter electrode in chronoamperometry mode

- ^aThe estimation was done with 14.3 mM DMSO in deuterated acetonitrile as the internal standard with the 3.9 ppm peak of caffeine and 4.1 ppm peak of **I**
- ^bThe estimation was done with 14.3 mM DFB in deuterated acetonitrile as the internal standard with ~63 ppm peak of **I** and ~79 ppm and ~88 ppm for the CF₃SO₂Na

Table S8: Summary of the results based on the parameters generated with the first iteration of the ML-assisted optimisation (**batch_1**)

Serial Number	Flow rate	ON Current	OFF Current	Duty cycle	<i>T</i>	<i>F</i>	¹ H NMR unreacted Caffeine ^a	¹ H NMR CF ₃ product ^a	¹⁹ F NMR unreacted CF ₃ SO ₂ Na ^b	¹⁹ F NMR product ^b	Yield	Production rate	pH
	mL min ⁻¹	mA	mA		°C	Hz	mM	mM	mM	mM	%	μmol min ⁻¹	
1	0.25	40.00	-80.00	0.99	65.00	100.00	25.28	20.66	31.96	18.79	41.68	4.29	2.20
2	0.25	40.00	-80.00	0.94	65.00	100.00	29.40	19.63	41.24	18.44	40.21	4.05	1.36
3	0.25	53.84	-57.16	0.99	65.00	100.00	21.25	25.10	28.31	23.48	51.32	7.31	2.40
4	0.25	40.00	-80.00	0.94	59.98	100.00	22.76	19.04	42.62	17.65	38.76	5.72	1.42
5	0.27	40.00	-7.66	0.99	65.00	59.95	24.34	19.28	51.25	18.80	40.22	6.55	1.66
6	0.25	80.00	23.50	0.94	65.00	100.00	18.40	22.13	9.85	22.65	47.31	6.82	0.52
7	2.00	80.00	-80.00	0.96	65.00	100.00	40.17	5.41	63.22	5.08	11.09	10.04	2.17
8	2.00	45.93	-80.00	0.90	64.91	98.70	44.16	3.41	73.20	3.01	6.78	5.70	1.86
9	1.94	40.00	-80.00	0.89	65.00	100.00	44.18	2.41	72.25	2.23	4.90	3.64	1.74
10	2.00	80.00	40.00	0.50	65.00	100.00	42.04	5.15	67.34	4.77	10.48	8.01	1.39
11	2.00	80.00	40.00	0.82	65.00	5.42	41.18	5.72	65.81	5.44	11.79	11.63	1.20
12	1.74	40.00	-80.00	0.93	65.00	70.25	42.61	3.43	73.73	3.34	7.15	6.27	0.87
13	1.34	49.76	30.23	0.92	55.24	53.07	40.36	6.03	64.26	5.71	12.40	9.29	1.99
14	0.45	47.49	33.46	0.96	19.48	100.00	34.01	11.86	42.88	11.09	24.25	6.18	2.64
15	0.25	80.00	40.00	0.92	65.00	100.00	20.39	26.04	12.05	23.42	52.25	5.55	2.39
16	0.25	80.00	4.14	0.80	65.00	100.00	19.64	26.72	19.10	24.39	53.99	5.85	1.26
17	0.25	44.99	-21.18	0.81	65.00	100.00	28.08	12.75	55.34	12.19	26.36	2.76	2.80

- All reactions were done with 100 mM TBAP in 10:1 acetonitrile: H₂O as electrolyte with Graphite as the working electrode and BCC-6mm SS as the counter electrode in chronoamperometry mode
- ^aThe estimation was done with 14.3 mM DMSO in deuterated acetonitrile as the internal standard with the 3.9 ppm peak of caffeine and 4.1 ppm peak of **I**
- ^bThe estimation was done with 14.3 mM DFB in deuterated acetonitrile as the internal standard with ~63 ppm peak of **I** and ~79 ppm and ~88 ppm for the CF₃SO₂Na

Table S9: Summary of the results based on the parameters generated with the second iteration of the ML-assisted optimisation (**batch_2**)

No	Flow rate	ON Current	OFF Current	Duty cycle	<i>T</i>	<i>F</i>	¹ H NMR unreacted Caffeine ^a	¹ H NMR CF ₃ product ^a	¹⁹ F NMR unreacted CF ₃ SO ₂ Na ^b	¹⁹ F NMR product ^b	Yield	Production rate	pH
	mL min ⁻¹	mA	mA		°C	Hz	mM	mM	mM	mM	%	μmol min ⁻¹	
1	0.25	80.00	15.50	0.82	65.00	100.00	23.17	16.59	19.27	15.64	35.11	4.76	1.90
2	0.25	80.00	30.71	0.83	65.00	100.00	16.87	21.16	9.25	20.89	45.81	6.78	1.70
3	0.25	80.00	40.00	0.82	65.00	100.00	24.88	16.87	14.59	15.55	35.31	5.02	1.50
4	0.25	80.00	40.00	0.83	65.00	100.00	24.31	19.16	11.83	17.65	40.09	5.69	1.40
5	0.25	80.00	40.00	0.83	65.00	100.00	22.31	18.30	9.92	17.74	39.26	4.98	1.30
6	1.90	80.00	40.00	0.99	65.00	0.10	37.75	5.15	67.05	4.86	10.91	11.01	2.30
7	2.00	80.00	40.00	1.00	65.00	0.10	32.60	3.72	67.24	4.86	9.35	9.39	2.90
8	1.92	80.00	40.00	1.00	65.00	0.50	40.33	5.43	67.05	5.25	11.63	11.23	3.00
9	2.00	80.00	40.00	0.99	65.00	0.15	34.89	4.00	69.63	4.96	9.76	9.78	3.20
10	2.00	80.00	40.00	0.98	65.00	0.10	41.76	4.00	71.25	4.86	9.66	9.96	3.30
11	2.00	80.00	40.00	0.97	65.00	0.10	40.04	4.00	70.68	4.96	9.76	10.18	3.20
12	0.25	80.00	40.00	0.83	65.00	100.00	18.88	19.73	8.39	18.79	41.96	5.82	2.40
13	0.25	80.00	40.00	0.83	65.00	100.00	18.59	20.59	8.30	19.17	43.31	4.39	2.10
14	0.25	80.00	40.00	0.83	65.00	100.00	19.73	22.02	10.02	20.70	46.53	6.84	2.10
15	0.25	80.00	40.00	0.82	65.00	100.00	18.88	21.16	9.92	20.51	45.39	6.56	2.10

- All reactions were done with 100 mM TBAP in 10:1 acetonitrile: H₂O as electrolyte with Graphite as the working electrode and BCC-6mm SS as the counter electrode in chronoamperometry mode
- ^aThe estimation was done with 14.3 mM DMSO in deuterated acetonitrile as the internal standard with the 3.9 ppm peak of caffeine and 4.1 ppm peak of **I**
- ^bThe estimation was done with 14.3 mM DFB in deuterated acetonitrile as the internal standard with ~63 ppm peak of **I** and ~79 ppm and ~88 ppm for the CF₃SO₂Na

Table S10: Estimated total Faradaic Efficiency (FE), including possible electron consumption from caffeine oxidation.

Total caff. added	Total unreacted caff.	Total I^a	Missing caff.	FE^b of CF₃ decomposition	FE of caff. degradation	Total FE
mM	mM	mM	mM	%	%	%
47.33	25.28	19.73	2.32	43.04%	8.61%	51.64%
47.33	21.25	24.29	1.79	42.34%	6.06%	48.40%
47.33	22.76	18.35	6.22	43.75%	30.45%	74.20%
47.33	24.34	19.04	3.95	34.32%	19.97%	54.29%
47.33	18.40	22.39	6.54	40.61%	15.49%	56.10%
47.33	40.17	5.25	1.91	62.97%	31.78%	94.75%
47.33	44.18	2.32	0.82	51.53%	27.69%	79.21%
47.33	42.04	4.96	0.33	56.76%	6.72%	63.48%
47.33	41.18	5.58	0.56	55.93%	10.06%	65.99%
47.33	42.61	3.39	1.33	35.43%	40.46%	75.88%
47.33	40.36	5.87	1.10	65.64%	20.40%	86.04%
47.33	34.01	11.48	1.84	59.61%	12.34%	71.95%
47.33	20.39	24.73	2.20	32.35%	4.30%	36.66%
47.33	19.64	25.55	2.14	34.72%	5.01%	39.73%
47.33	28.08	12.47	6.77	23.46%	27.58%	51.05%
45.903	23.166	16.12	6.62	59.76%	24.51%	84.27%
45.903	16.874	21.03	8.00	69.76%	29.94%	99.70%
45.903	24.882	16.21	4.81	61.97%	17.22%	79.19%
45.903	24.31	18.40	3.19	64.37%	11.40%	75.77%
45.903	22.308	18.02	5.57	61.75%	18.62%	80.37%
45.903	40.326	5.34	0.24	74.19%	4.19%	78.38%
45.903	40.04	4.48	1.38	61.35%	25.75%	87.10%
45.903	18.876	19.26	7.76	66.53%	27.39%	93.92%
45.903	18.59	19.88	7.43	54.64%	21.50%	76.14%
45.903	19.734	21.36	4.81	67.26%	17.53%	84.78%
45.903	18.876	20.84	6.19	66.90%	22.41%	89.32%

- ^aRefers to the product, **I**
- ^bFaradaic efficiency is abbreviated to FE

S8: Kinetics Modelling

We visualise the 30 Latin hypercube data points to gain intuition about how each controlled condition affects the species concentrations at the outlet. As we can see on **Figure S13A**, the two strongest influencing factors for yield are residence time and temperature. In contrast, the current has a relatively weak effect and the role played by pulsing on yields is relatively ambiguous (**Figure S13B**).

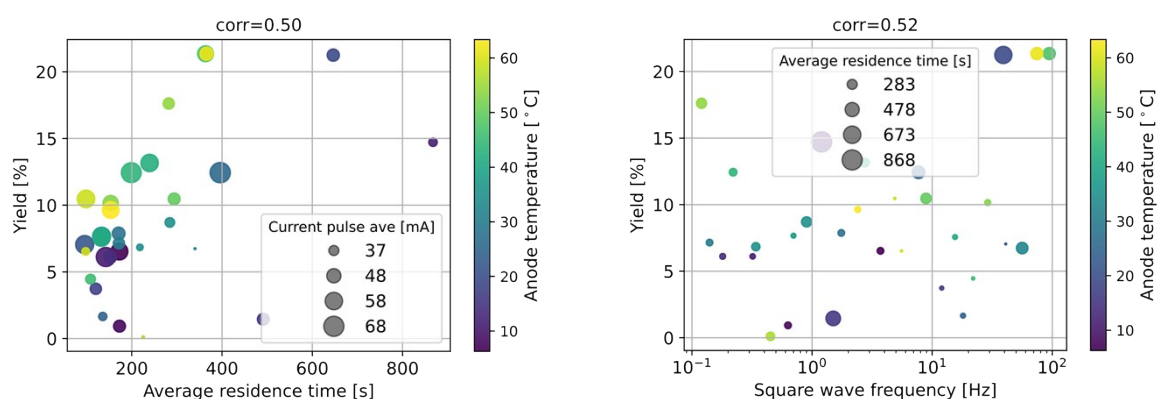


Figure S12: Visualising the experimental data obtained from 30 Latin-hypercube flow reactor runs between (left) flow rate, temperature, and current magnitude and (right) pulsing frequency, current magnitude, and temperature. Yield is defined as the ratio of the final **I** concentration to the initial caffeine concentration.

In **Figure S14**, we visualise the extent of side reactions by comparing the amounts of reacted reactants to that of products. The left panel indicates that reacted caffeine roughly matches **I**, so its side reaction is quite mild. In contrast, the right plot shows that reacted NaSO_2CF_3 is typically twice to four times as much as **I**, aligned with the common practice of using twice as much NaSO_2CF_3 as the substrate in the beginning. The obvious candidates for such side reactions include the dimerisation of the CF_3^\bullet and the formation of CHF_3 from CF_3^\bullet and H^\bullet , as mentioned before.

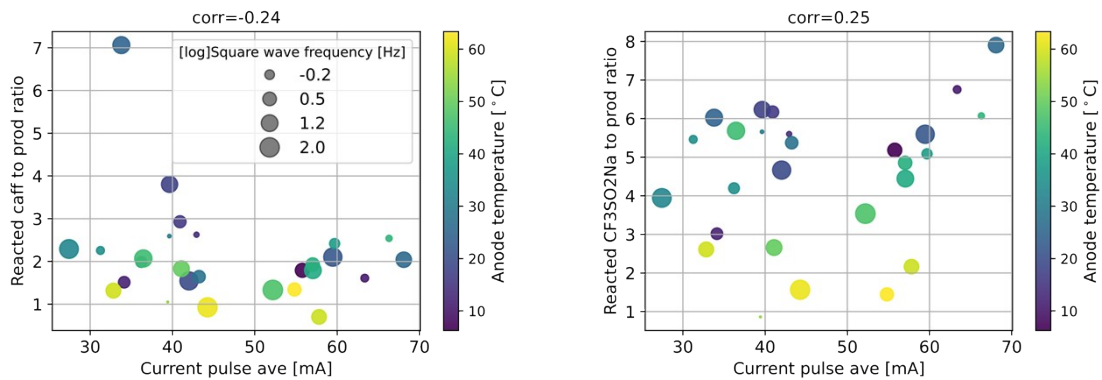


Figure S13: Visualising extent of side reactions. Reacted caffeine is compared to **I** on the left, while reacted NaSO_2CF_3 against **I** on the right.

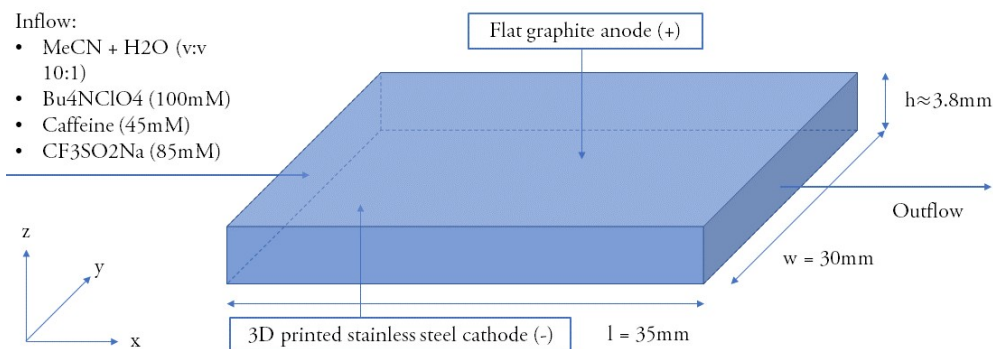


Figure S14: Schematic of the flow cell reactor for trifluoromethylation of caffeine.

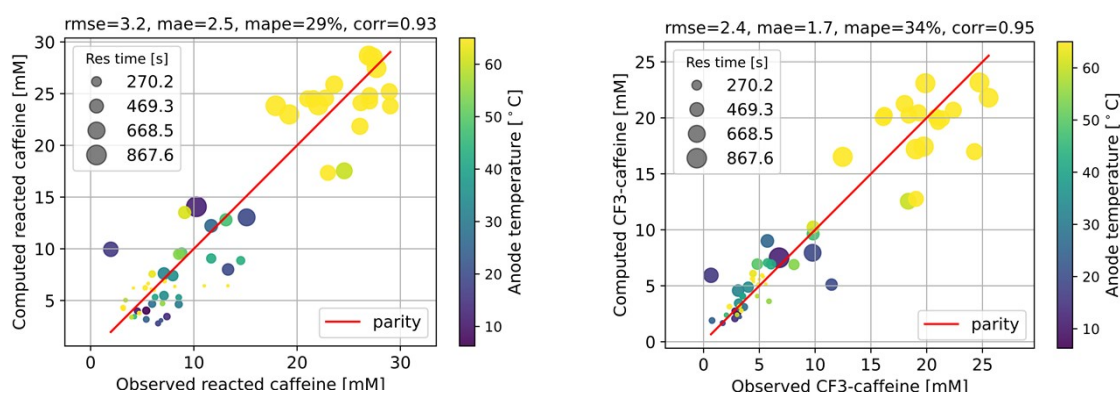


Figure S15: Fitting the kinetic parameters of the full reaction network.

S9 Caution on the use of TBAP:

Like many other perchlorates, the supporting electrolyte used in this work, TBAP, is a strong oxidiser and hazardous chemical. In this work, TBAP was used as supporting electrolyte to reduce electrochemical resistance, which allows us to observe small redox signals more clearly. Care must be taken that it is used only under strength <1 M. inside a fumehood with no potential sources of ignition present in the vicinity. A type B fire extinguisher is suggested for small fires, and evacuation of the premises is advisable for any large fires involving perchlorates.

We envision that in larger scale electrosynthesis, TBAP will not be necessary as the increased reagent concentration will be able to provide sufficient ionic conductivity.

S9: References:

- 1 F. Malz and H. Jancke, *J. Pharm. Biomed. Anal.*, 2005, **38**, 813–823.
- 2 M. D. McKay, R. J. Beckman and W. J. Conover, *Technometrics*, 1979, **21**, 239.
- 3 scikit-optimize: sequential model-based optimisation in Python — scikit-optimize 0.8.1 documentation, <https://scikit-optimize.github.io/stable/>, (accessed 8 March 2023).
- 4 Keras-Team, keras: Deep Learning for humans, <https://github.com/fchollet/keras>, (accessed 4 March 2023).